Magnetic structure of GdAgSb$_2$ determined by x-ray resonant exchange scattering

C. Song, W. Good, D. Wermeille, A. I. Goldman, S. L. Bud'ko, and P. C. Canfield

Ames Laboratory–US DOE and Department of Physics and Astronomy, Iowa State University, Ames, Iowa 50011

X-ray resonant exchange-scattering experiments were performed on a single crystal of GdAgSb$_2$ to determine the magnetic structure. Long-range antiferromagnetic ordering, characterized by a wave vector of $\vec{\tau} = (\frac{1}{2}00)$, develops below the Néel temperature ($T_N = 13$ K), consistent with the dc susceptibility measurements. For the scattering geometry employed in these measurements, the resonant enhancement at the $(\frac{1}{2}08)$ magnetic peak arises from electric quadrupole transitions only while the resonant enhancement at the $(0-\frac{1}{2}8)$ magnetic peak arises from electric dipole transitions. Q-dependent integrated intensity measurements were carried out, along with polarization analysis of the scattered beam, and demonstrated that the moments lie in the tetragonal basal plane and are perpendicular to the magnetic wave vector.

PACS number(s): 75.25.+z, 75.50.−y, 75.50.Ee

The recent availability of high quality single crystal samples of the RAgSb$_2$ (R=rare-earth ion) compounds has stimulated new interest in the highly anisotropic electronic and magnetic properties of these materials and their manifestation in various physical phenomena.[1,2] Along with some generic features reported for the members of this family of compounds, some display exotic low-temperature physical properties as well. For example, CeAgSb$_2$ displays Kondo lattice behavior,[3] with ground-state ferromagnetism. DyAgSb$_2$ exhibits 11 well-defined metamagnetic transitions in applied field at low temperature.[4]

Most of the RAgSb$_2$ compounds display long-range antiferromagnetic ordering at low temperature.[5] The reported transition temperatures, for the heavy rare-earth compounds, scale with the de Gennes factor indicating that the Ruderman-Kittel-Kasuya-Yoshida (RKKY) interaction is the primary exchange interaction between local moments of the rare-earth ions.[1,5] For the light rare-earth compounds, however, there are significant deviations from de Gennes scaling which are claimed to result from the influence of strong crystalline electric-field (CEF) effects.[5] Indeed, these authors have noted that the incommensurate magnetic structure found in NdAgSb$_2$ is consistent with the predominance of the RKKY-type exchange interaction over CEF effects in this case.

Due to the fact that the orbital angular momentum $L=0$ for the $4f$ orbitals of Gd, GdAgSb$_2$ should be free of CEF effects. A determination of the magnetic structure of this system, then, can help to resolve issues regarding the role of CEF effects on magnetic ordering in this family of compounds. The extensive neutron scattering experiments on powder samples of RAgSb$_2$ compounds reported by André *et al.*,[5] however, did not include the Gd compound, presumably because of the neutron opacity of the naturally abundant Gd ion.[8]

In this paper, we report on the magnetic structure of GdAgSb$_2$ determined from x-ray resonant exchange-scattering measurements performed on a single crystal. GdAgSb$_2$, along with other family members, crystallizes in the tetragonal ZrCuSi$_2$-type structure (space group $P4/nmm$) with the Gd ions at the $2c$ positions[6,7] as shown in Fig. 1. For this compound, antiferromagnetism was reported from

the bulk susceptibility measurements with a transition temperature of $T_N = 12.8$ K. Our results show that below $T_N \approx 13$ K, GdAgSb$_2$ orders in a commensurate antiferromagnetic structure with a wave vector of $\vec{\tau} = (\frac{1}{2}00)$. The magnetic unit cell is twice the chemical unit cell along one of the basal plane axes. From measurements of the Q dependence of the integrated intensity as well as from a polarization analysis of the scattered beam, we show that the moments
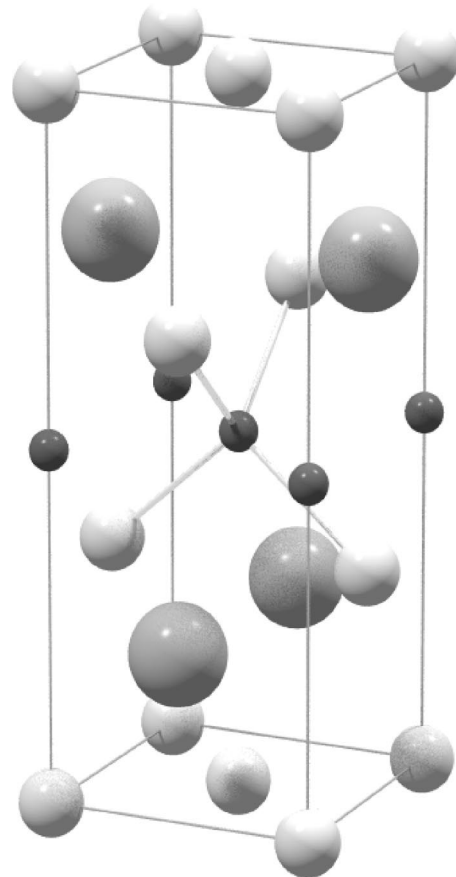

FIG. 1. The crystal structure of GdAgSb$_2$ ($P4/nmm$, No. 129). The large dark gray circles represent Gd ions, the medium light gray circles represent Sb, and the small black circles represent Ag.

are confined to the basal plane, and transverse to the ordering wave vector.

Single crystals of GdAgSb$_2$ were grown using a high-temperature flux technique at the Ames Laboratory.[9] The resulting crystals are shaped as platelets with the flat surface perpendicular to the crystallographic $\hat{c}$ direction (the [00l] unique axis of the tetragonal structure). Further polishing of the sample surface was not possible without degrading the sample quality (increasing the sample mosaicity) due to its softness. For the magnetic x-ray-diffraction experiment, the cleanest sample, without noticeable flux inclusions from the growth process, was chosen. For this sample, the mosaic was measured to be 0.015° at the (008) reflection.

The resonant x-ray scattering experiments were carried out on the 6-ID undulator beam line in the Midwest University Collaborative Access Team (MUCAT) sector at the Advanced Photon Source using a double-crystal Si(111) monochromator. Polarization analysis of the scattered radiation was accomplished by using a pyrolytic graphite (PG) (006) analyzer set to scatter in the horizontal plane (perpendicular to the sample scattering plane). In this configuration, the analyzer scattering angle is close to 90° at the Gd L_{III} absorption edge, and the $\vec{\sigma}$-polarized component (polarization vector out of the sample scattering plane) of the scattered radiation is effectively suppressed by the analyzer. By moving from the PG(006) reflection to the PG(002) reflection, the analyzer scattering angle changes from 99.6° to 29.5°, allowing the $\vec{\sigma}$-polarized component to pass as well.

The single crystal of GdAgSb$_2$ was mounted on a copper rod, using silver paint, and wrapped with 15-μm aluminum foil to ensure good thermal contact. The Cu rod was attached to the cold finger of a closed cycle displex cryogenic refrigerator. The sample was oriented with the (h0l) zone in the scattering plane. The polarization of the incident beam (predominantly $\vec{\sigma}$ polarized) was perpendicular to the scattering plane {parallel to the [0k0] direction for any (h0l) reflection}. As discussed by Hill and McMorrow, in this configuration the resonant scattering that arises from electric dipole transitions (E1) is $\vec{\pi}$ polarized and sensitive only to the component of the magnetic moment in the (h0l) plane (ac plane).[10] The measured intensity is proportional to $(z_h \cos\theta + z_l \sin\theta)^2$, where z_h and z_l are components of the magnetic moment along the [h00] and [00l] directions, respectively. On the other hand, the $\vec{\sigma}$-polarized component of the scattered radiation can arise from both nonresonant and electric quadrupole (E2) transitions, and is sensitive to the component of the magnetic moment along [0k0]. By a straightforward change in the analyzer angle from the PG(006) to PG(002) reflection, then, both the in-plane and out-of-plane components of the magnetic moment can be probed.

After an extensive search for the magnetic peak in the $\vec{\pi}$-polarized scattering from the sample, no signal could be found. However, as shown in Fig. 2, after changing the scattering angle of the analyzer crystal to make use of the PG(002) reflection, allowing both $\vec{\sigma}$ and $\vec{\pi}$ scattering to pass, magnetic peaks were observed at positions corresponding to $\vec{\tau} = (\frac{1}{2}00)$. This result indicates that (i) the ordered moment
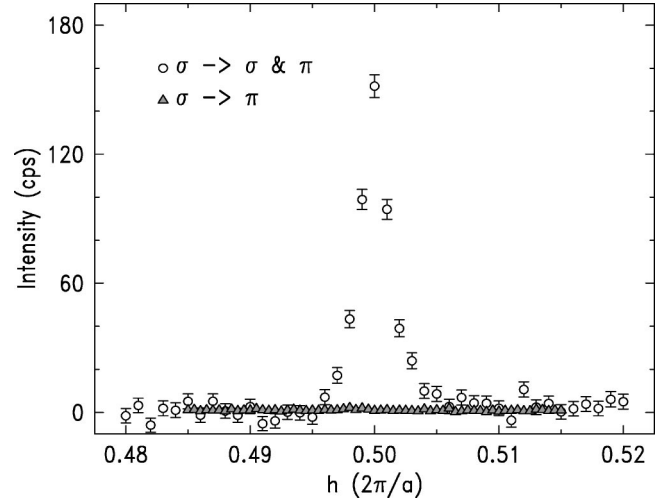

FIG. 2. Reciprocal space scan with polarization analysis using the PG analyzer crystal at the $(\frac{1}{2}08)$ magnetic satellite peak of GdAgSb$_2$ at 8 K. The extinction of the magnetic signal in the $\vec{\sigma}$-to-$\vec{\pi}$ channel is clearly observed.

direction in the antiferromagnetic state is oriented out of the scattering plane transverse to the magnetic wave vector, and (ii) any resonant scattering enhancement in this geometry arises from electric quadrupole (E2) rather than dipole (E1) transitions.

In order to confirm that the observed scattering at $\vec{\tau} = (\frac{1}{2}00)$ arises from quadrupole resonant scattering, energy scans through the Gd L_{III} absorption edge were done at sev-
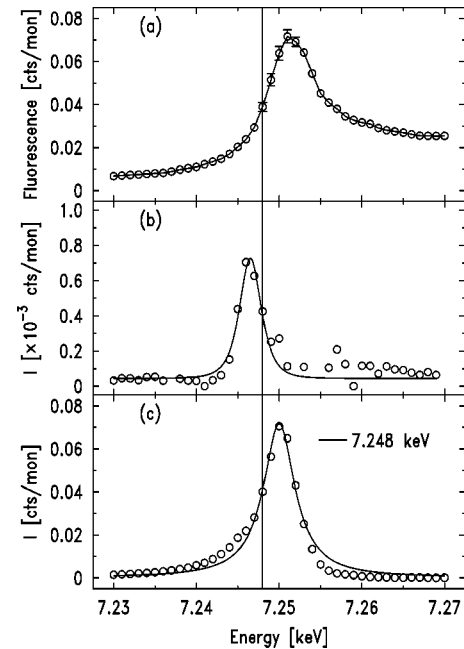

FIG. 3. Energy scans through the Gd L_{III} edge of GdAgSb$_2$ at $T = 6$ K showing (a) the background fluorescence from the sample, (b) the resonant scattering enhancement at the $(\frac{1}{2}08)$ magnetic satellite, and (c) the resonant enhancement of the $(0-\frac{1}{2}8)$ magnetic satellite.
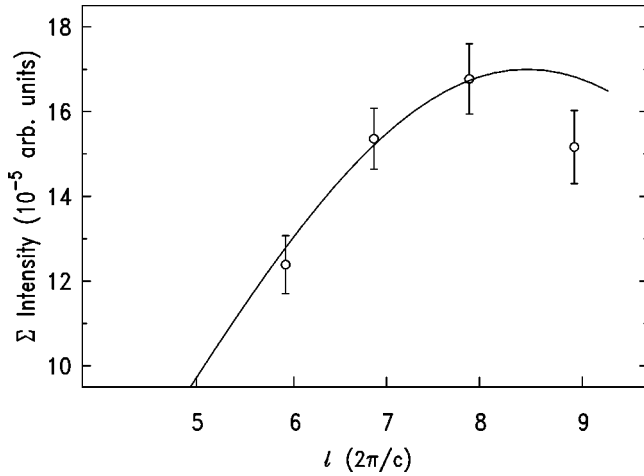
FIG. 4. Q-dependent integrated intensities of $(\frac{1}{2}0l)$ magnetic satellites of GdAgSb$_2$ at 8 K. The solid line is the calculated $E2$ cross section for a moment direction along $[0k0]$.

FIG. 5. The temperature dependence of the integrated intensity of $(\frac{1}{2}08)$ magnetic satellites of GdAgSb$_2$. The solid line is a fit of the data to a power-law fit as described in the text.

eral magnetic satellite peaks. Figure 3(a) shows the energy profile of the fluorescence background from the sample that is used to define the energy position of the absorption edge. The resonant enhancement observed at the magnetic satellite position $[(\frac{1}{2}08)]$ is shown in Fig. 3(b). The solid line here represents a fit of the data to a Lorentzian squared line shape. As clearly shown by the vertical line in the figure, the peak of the resonance is found at an energy lower than the maximum in the derivative of the absorption edge (solid vertical line). This feature of a quadrupole resonance is commonly observed and arises from the strong attractive interaction between the core hole in the $2p_{3/2}$ orbital and an electron excited to the strongly localized $4f$ band.[11,12] We note that it should be possible to observe dipole resonant magnetic scattering by moving to a magnetic wave vector such as $(0 -\frac{1}{2}8)$. For this reflection, the moment direction, now along $(h00)$, lies in the scattering plane. Figure 3(c) shows energy scans through the Gd L_{III} edge at the $(0-\frac{1}{2}8)$ reflection, where we see that the peak of the dipole $(E1)$ resonance for this reflection lies above the absorption edge and is significantly stronger than that found for the $(\frac{1}{2}08)$ reflection. This is consistent with our original assignment of a quadrupole resonance for the $(\frac{1}{2}08)$ magnetic peak with the magnetic moment transverse to the magnetic wave vector.

Finally, to confirm that the resonant enhancement at the $(h/208)$ magnetic peak arises from electric quadrupole transitions with the moment transverse to the magnetic wave vector, as determined from the polarization analysis discussed above, Q-dependent integrated intensity measurements were performed using those magnetic peaks, $(\frac{1}{2}0l)$, that could be accessed in the symmetric scattering geometry.[13] The integrated intensity was measured with open detector slits using the PG(002) reflection from the analyzer crystal. The rather broad mosaic of the analyzer, $\sim 0.5°$, is significantly larger than the full width at half maximum of magnetic satellites of $\sim 0.1°$, ensuring adequate integration of the scattered intensity. Proper integration over 2θ and χ was achieved by opening the detector slits until a flat top was
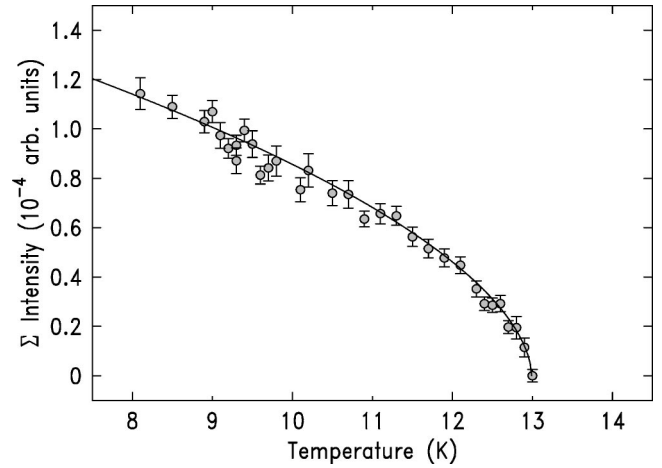
observed in 2θ and χ scans through the magnetic peaks. The integrated intensity of these satellite peaks was calculated from rocking scans of the sample crystal through the magnetic reflections. The observed integrated intensities of the magnetic satellites are plotted in Fig. 4. The solid line in Fig. 4 represents a fit to the theoretical quadrupole resonance scattering cross section with the moment direction along $[0k0]$ showing reasonable agreement with the data.[10,14]

The temperature dependence of the integrated intensity $(I \sim \mu^2)$ of the $(\frac{1}{2}08)$ magnetic satellite peak at the L_{III} resonance energy is displayed in Fig. 5. The solid line is a fit to the power law, $I \sim \mathcal{A}(T_N - T)^{2\beta}$. A transition temperature, $T_N = 13.0$ K, obtained from the fit, is close to the value $T_N = 12.8$ K obtained from the bulk susceptibility measurement.[1]

The principal result of this work is the *ab initio* determination of the magnetic structure of GdAgSb$_2$ by x-ray resonant exchange scattering. Below 13 K, the local magnetic moments order antiferromagnetically, doubling the unit cell along the $\vec{a}$ direction (or equivalently in the tetragonal structure's $\vec{b}$ direction) in the basal plane, with the moments ordered transverse to this direction also within the basal plane. These results then indicate that the commensurate antiferromagnetic ordering observed in several of the RAgSb$_2$ compounds is not necessarily driven by the strong CEF effects as proposed by Andre *et al.*[5] Indeed, it should be noted that in the related RNi$_2$B$_2$C family, the Gd compound, as well as many of the strongly anisotropic member compounds (R =Er, Tb, Ho), orders in an incommensurate structure determined largely by Fermi-surface nesting.[15,16] The interactions that conspire to produce magnetic ordering in many of these systems are quite complex, involving the RKKY-type indirect exchange, CEF anisotropies, and, especially for the light rare-earth ions, hybridization effects and possible changes in the indirect exchange coupling. Clearly, a great deal of further study is necessary to unravel the contributions of all of these mechanisms.

---

[1] K. D. Meyers, S. L. Bud'ko, I. R. Fisher, Z. Islam, H. Kleinke, A. H. Lacerda, and P. C. Canfield, J. Magn. Magn. Mater. **205**, 27 (1999).

[2] K. D. Meyers, S. L. Bud'ko, V. Antropov, B. N. Harmon, and P. C. Canfield, Phys. Rev. B **60**, 13 371 (1999).

[3] M. J. Thornton, J. G. M. Armitage, G. J. Tomka, P. C. Reidi, R. H. Mitchel, M. Houshiar, D. T. Adroja, B. D. Rainford, and D. Fort, J. Phys.: Condens. Matter **10**, 9485 (1998).

[4] K. D. Meyer, P. C. Canfield, V. A. Kalatsky, and V. L. Pokrovsky, Phys. Rev. B **59**, 1121 (1999).

[5] G. André, F. Bourée, M. Kolenda, B. Leśniewska, A. Oleś, and A. Szytula, Physica B **292**, 176 (2000).

[6] M. Brylak, M. H. Möller, and W. Jeitschko, J. Solid State Chem. **115**, 305 (1995).

[7] O. Sologub, H. Noël, A. Leithe-Jasper, P. Rogl, and O. I. Bodak, J. Solid State Chem. **115**, 441 (1995).

[8] G. E. Bacon, *Neutron Diffraction*, 3rd ed. (Oxford University, New York, 1975), p. 73.

[9] P. C. Canfield and Z. Fisk, Philos. Mag. B **56**, 7843 (1992).

[10] J. P. Hill and D. F. McMorrow, Acta Crystallogr., Sect. A: Found. Crystallogr. **52**, 236 (1996).

[11] Paolo Carra, B. N. Harmon, B. T. Thole, M. Altarelli, and G. A. Sawatzky, Phys. Rev. Lett. **66**, 2495 (1991).

[12] X. Wang, T. C. Leung, B. N. Harmon, and P. Carra, Phys. Rev. B **47**, 9087 (1993).

[13] C. Detlefs, Z. Islam, A. I. Goldman, C. Stassis, P. C. Canfield, J. P. Hill, and D. Gibbs, Phys. Rev. B **55**, R680 (1997).

[14] M. D. Hamrick, Ph.D. thesis, Rice University, 1994.

[15] J. W. Lynn, S. Skanthakumar, Q. Huang, S. K. Sinha, Z. Hossain, L. C. Gupta, R. Nagarajan, and C. Godart, Phys. Rev. B **55**, 6584 (1997).

[16] C. Stassis and A. I. Goldman, J. Alloys Compd. **250**, 603 (1997).